

Solar modulation of galactic hydrogen and helium over the 23rd solar minimum with the PAMELA experiment

V. DI FELICE¹, M. BOEZIO², A. BRUNO^{3,4}, N. DE SIMONE¹, V. FORMATO^{2,5}, N. MORI⁶, E. VANNUCCINI⁶, O. ADRIANI^{6,7}, G. C. BARBARINO^{8,9}, G. A. BAZILEVSKAYA¹⁰, R. BELLOTTI^{3,4}, E. A. BOGOMOLOV¹¹, M. BONGI^{6,7}, V. BONVICINI², S. BOTTAI⁶, F. CAFAGNA³, D. CAMPANA⁹, R. CARBONE², P. CARLSON¹², M. CASOLINO^{1,13}, G. CASTELLINI¹⁴, C. DE DONATO¹, M.P. DE PASCALE^{1,15,*}, C. DE SANTIS^{1,15}, A. M. GALPER¹⁶, A. V. KARELIN¹⁶, S. V. KOLDASHOV¹⁶, S. KOLDOBSKIY¹⁶, S. Y. KRUTKOV¹¹, A. N. KVASHNIN¹⁰, A. LEONOV¹⁶, V. MALAKHOV¹⁶, L. MARCELLI¹⁵, M. MARTUCCI^{15,17}, A. G. MAYOROV¹⁶, W. MENN¹⁸, M. MERGÈ^{1,15}, V. V. MIKHAILOV¹⁶, E. MOCCHIUTTI², A. MONACO³, R. MUNINI^{2,5}, G. OSTERIA⁹, F. PALMA^{1,15}, P. PAPINI⁶, M. PEARCE¹², P. PICOZZA^{1,15}, C. PIZZOLOTTO^{19,20,†}, M. RICCI¹⁷, S. B. RICCIARINI⁶, R. SARKAR², V. SCOTTI^{8,9}, M. SIMON¹⁸, R. SPARVOLI^{1,15}, P. SPILLANTINI^{6,7}, Y. I. STOZHKOVA¹⁰, A. VACCHI², G. VASILYEV¹¹, S. A. VORONOV¹⁶, Y. T. YURKIN¹⁶, G. ZAMPA², N. ZAMPA², V. G. ZVEREV¹⁶, M.S. POTGIETER²¹, R. DU T. STRAUSS²¹, E.E. VOS²¹.

¹ INFN, Sezione di Roma "Tor Vergata", I-00133 Rome, Italy

² INFN, Sezione di Trieste, I-34149 Trieste, Italy

³ INFN, Sezione di Bari, I-70126 Bari, Italy

⁴ University of Bari, Department of Physics, I-70126 Bari, Italy

⁵ University of Trieste, Department of Physics, I-34147 Trieste, Italy

⁶ INFN, Sezione di Florence, I-50019 Sesto Fiorentino, Florence, Italy

⁷ University of Florence, Department of Physics, I-50019 Sesto Fiorentino, Florence, Italy

⁸ University of Napoli "Federico II", Department of Physics, I-80126 Naples, Italy

⁹ INFN, Sezione di Napoli, I-80126 Naples, Italy

¹⁰ Lebedev Physical Institute, RU-119991, Moscow, Russia

¹¹ Ioffe Physical Technical Institute, RU-194021 St. Petersburg, Russia

¹² KTH, Department of Physics, and the Oskar Klein Centre for Cosmoparticle Physics, AlbaNova University Centre, SE-10691 Stockholm, Sweden

¹³ RIKEN, Advanced Science Institute, Wako-shi, Saitama, Japan

¹⁴ IFAC, I-50019 Sesto Fiorentino, Florence, Italy

¹⁵ University of Rome "Tor Vergata", Department of Physics, I-00133 Rome, Italy

¹⁶ NRNU MEPhI, RU-115409 Moscow, Russia

¹⁷ INFN, Laboratori Nazionali di Frascati, Via Enrico Fermi 40, I-00044 Frascati, Italy

¹⁸ Universitat Siegen, Department of Physics, D-57068 Siegen, Germany

¹⁹ INFN, Sezione di Perugia, I-06123 Perugia, Italy

²⁰ Agenzia Spaziale Italiana (ASI) Science Data Center, I-00044 Frascati, Italy

²¹ North-West University, Centre for Space Research, 2520 Potchefstroom, South Africa

(*) Deceased

(†) Previously at INFN, Sezione di Trieste, I-34149 Trieste, Italy

valeria.difelice@roma2.infn.it

Abstract: PAMELA has been orbiting the Earth for more than six years, gathering data on solar, galactic and trapped cosmic rays during the time of the last solar minimum. The apparatus comprises a time-of-flight system, a silicon-microstrip magnetic spectrometer, a silicon-tungsten electromagnetic calorimeter, an anticoincidence system, a shower tail catcher scintillator and a neutron detector. The combination of these devices allows charged particle and antiparticle identification over a wide energy range and with an unprecedented precision. The quasi-polar orbit of the instrument, with an inclination of 70 degrees, makes it possible to measure low energy particles starting from about 100 MeV/n. In this work we present the time and rigidity dependence of the galactic proton and helium fluxes over the first 4 years of operation during the $A < 0$ solar minimum of solar cycle 23.

Keywords: cosmic rays, solar modulation, satellite-borne experiment

1 Introduction

PAMELA, Payload for Matter-Antimatter Exploration and Light Nuclei Astrophysics, is a satellite-borne experiment designed to make long duration measurements of the cosmic radiation. The instrument is optimized to detect charged particles and antiparticles in an energy range from tens of MeV to TeV, with the main aim to search for primordial

antimatter, signals from dark matter annihilation and exotic matter. PAMELA is also measuring with great accuracy the absolute fluxes of primary and secondary cosmic rays (CRs). In particular, PAMELA has provided proton and helium energy spectra measurements [1, 2] in the range of energy between 80 MeV - 1.2 TeV and 1 GeV - 450 GeV, respectively. For the first time such an extended energy range has been explored by a single instrument, allowing to over-

come issues in data comparison and interpretation related to different instrumental systematics. The measurement results clearly evidence interesting features in the high energy part of the spectra, giving fundamental contributions to the study of the particle acceleration and propagation in the Galaxy. At energies below ~ 30 GeV, PAMELA measurements differ from those from other instruments. The different periods of solar activity in which data have been collected from the various experiments could explain these differences.

Indeed, the Sun assumes a very important role for missions aiming to detect charged particles in space, not only being a powerful particle source, but also influencing the propagation of galactic particles that interact, traveling through the heliosphere, with the solar wind and the embedded magnetic field. The resulting solar modulation distorts the spectral shape and intensity below 50 GeV depending on particle energy, type, sign of charge and position in the heliosphere. The flux intensity also varies with time in anti-correlation with the solar activity, making galactic charged particle spectra a valuable indicator of it. Solar activity follows a cycle of approximately 11 years, rising from a minimum, when the Sun is quiet, to a maximum, characterized by a turbulent heliospheric environment, then returning to a minimum. At each maximum of solar activity the polarity of the solar magnetic field reverses, causing the well known 22-years solar activity cycle observed in neutron monitor counts [3, 4]. In particular, the last $A < 0$ solar cycle has been very peculiar, being one of the deepest and stable solar minima in almost a century, thus offering ideal conditions for solar modulation studies [5]. Information provided by accurate measurements of low energy cosmic rays are necessary for a better understanding of the solar environment, interesting in their own right and essential for the modeling of possible primary signal background [6].

PAMELA has been measuring cosmic rays during this last remarkable solar minimum, going toward the solar maximum of current cycle 24. The instrument, installed on board of the Resurs-DK1 satellite, has been launched the 15th of June 2006 and it is still operating, daily delivering to Earth 16 Gigabytes of data. Until September 2010, it has been following an elliptical orbit, at an altitude ranging between 350 – 610 km with an inclination of 70.0° , changed then to the current nearby circular one, at an altitude of ~ 570 km. Thanks to its orbital and instrumental characteristics and the long duration flight, PAMELA is measuring cosmic rays down to ~ 100 MeV. In this paper we discuss the energy spectra measurements of the most abundant components of galactic cosmic rays, hydrogen and helium, constituting about 98% of the total CR flux. We focus on the low energy particle intensity ranging from 80 MeV/n to some tens of GeV/n, where solar modulation is effective.

2 The PAMELA instrument

The core of the instrument is a magnetic spectrometer, constituted by a 0.43 T permanent magnet and a silicon tracking system. The 300 μm thick double-sided Si sensors of the tracking system measure two independent impact coordinates (bending X-view and non-bending Y-view) on each plane. The tracker provides the sign of the electric charge and a measure of the rigidity (momentum divided by charge), with a maximum detectable rigidity of 1.2 TV. The magnetic cavity defines the instrument geometric factor to

be 21.5 cm^2 sr. A system of six layers of plastic scintillators, arranged in three double planes (S1, S2 and S3), provides a fast signal for triggering the data acquisition. Moreover it measures the ionization energy loss and the Time of Flight (ToF) of traversing particles with a resolution of 300 ps, assuring charge particle absolute value determination and albedo particle rejection. An electromagnetic imaging W/Si calorimeter and a neutron counter allow particle identification, distinguishing between hadronic and electromagnetic components of cosmic rays. The total depth of the calorimeter is $16.3 X_0$ (0.6 nuclear interaction lengths). Thanks to its longitudinal and transverse segmentation, the calorimeter exploits the different development of electromagnetic and hadronic showers, allowing a rejection power of interacting and non-interacting hadrons at the order of 10^5 . A plastic scintillator, placed beneath the calorimeter, increases the identification of high-energy electrons. The neutron detector complements the electron-proton discrimination capabilities of the instrument by detecting the increased neutron production in the calorimeter associated with hadronic showers compared to electromagnetic ones. The whole instrument is surrounded by an anticoincidence system (AC) of three scintillators (CARD, CAS and CAT) for the rejection of background events. More detail can be found in Picozza et al. [7].

3 Hydrogen and Helium identification

In order to select a clean hydrogen and helium particle sample and to precisely reconstruct their rigidity, a precision track in the spectrometer was required, with a trajectory contained within the fiducial instrument acceptance. The trajectory was reconstructed by fitting the tracking system information. The goodness of the fit is defined in terms of χ^2 and depends on the number of points used for the track reconstruction. In particular, with respect to the previous hydrogen and helium analysis [1], the tracking conditions for hydrogen were relaxed by requiring at least 3 hits, instead of 4, on both X and Y view, and a track lever-arm of at least 4 silicon planes in the tracker; moreover, for both particles, the fiducial volume was enlarged (bounded 1.5 mm from the magnet cavity walls, instead of 7 mm), allowing to collect more particles with only a small degradation in

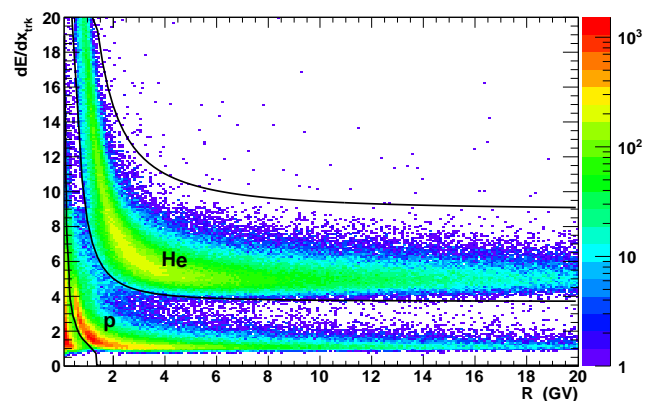


Figure 1: Energy released in the PAMELA tracker system by hydrogen and helium particles as a function of the particle rigidity.

the measurement precision in the energy range under study. Such changes of the analysis procedure aimed to maximize the statistics, in order to follow the spectral evolution in time (see [2]), while the previous study aimed to minimize systematic uncertainties and to maximize the spectrometer performances in order to obtain a precise flux measurement up to the highest achievable energy.

A further cleaning of the particle sample was required due to the presence of secondary low energy particles, mainly protons, generated from the interaction of primaries in the instrument, that constitute a source of eliminable background. They have been rejected by using the ToF, whose segmentation allowed to identify multiple particle events, and the anticoincidence system (CARD and CAT), being the latter not necessary in the helium measurement case. Then, particles with positive curvature and ionization energy losses in the tracking system compatible with hydrogen and helium have been selected. Figure 1 shows these particle populations and the corresponding selection bands, that also include hydrogen and helium isotopes.

Galactic particles were selected by requiring the measured rigidity to be a factor 1.3 above the geomagnetic vertical cutoff, evaluated using the Störmer approximation, at a given orbital position. The satellite orbital characteristics allow to study particle fluxes down to the minimum detectable rigidity, that is determined by the trigger condition: acquired events must cross the S2 and S3 scintillators, respectively located above and below the tracking system, thus limiting the minimum detectable rigidity to an average of 400 MV for protons and 760 MV for helium (vertical incidence).

4 Flux estimation

The absolute particle flux was obtained by dividing the measured energy spectrum by the acquisition time, the geometrical acceptance and the selection efficiencies. For each energy bin the acquisition time was evaluated as the live time spent above the geomagnetic cutoff, thus reducing the total live time to, e.g., about 25% of its value at ~ 1 GV. Moreover the time spent inside the South Atlantic Anomaly and the period of occurrence of the December 2006 solar event were excluded from the analyzed data set. The PAMELA geometrical factor for the fiducial acceptance, as defined above, is $19.9 \text{ cm}^2\text{sr}$.

A precise evaluation of the selection efficiencies, and in particular of their variation in time, was a crucial aspect of this analysis. The redundant information on the particle characteristics that the PAMELA detectors can provide have been used to measure the selection efficiencies directly from flight data and independently for each time interval. The major time dependent effect was due to the failure of some front-end chips in the tracking system, translating into a progressive reduction of the tracking efficiency, with no degradation in the signal-to-noise ratio and spatial resolution. The tracker efficiency measurement has involved the use of the calorimeter for the selection of the efficiency sample of not interacting particles. Simulation was used for the determination of the rigidity dependence of the tracking efficiency, not evaluable from flight data. Simulation results have been compared to those obtained from flight, including differences as part of the systematic uncertainties. The selection efficiency of the ToF system was also evaluated from flight, relative to the tracking system. Low energy secondary protons correlated the ToF and AC systems due to

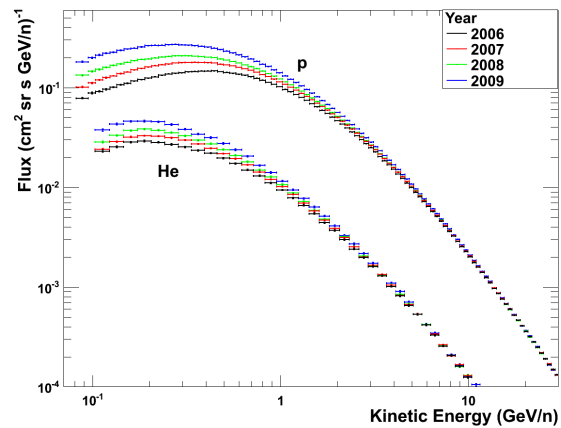


Figure 2: Hydrogen and preliminary helium yearly averaged spectra from 2006 to 2009.

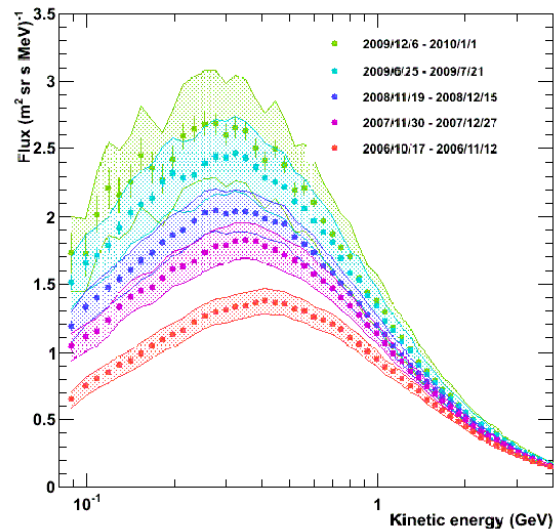


Figure 3: Proton flux measured by PAMELA during several time Carrington rotations from 2006 to the end of 2009.

background interactions associated to multiple hits in both scintillator systems. This resulted in the impossibility to perform a separate estimate of the two efficiencies and in an underestimation of the overall efficiency. The effect of these secondaries has been minimized removing most of them from the efficiency sample. The residual contamination has been accounted in an asymmetric systematic uncertainty found to be $\simeq 6\%$ in the lowest energy bin and to decrease down to a negligible value at about 1 GeV.

In order to correct for the particle energy losses inside the apparatus, particularly relevant at low energy, and to take into account the finite resolution of the spectrometer, an unfolding procedure was applied to the reconstructed spectra, following a Bayesian approach [8]. Moreover, the resulting hydrogen spectrum was then corrected for the contamination of locally produced secondary particles, that was found to be less than 6% at 0.4 GV, decreasing with increasing energy and becoming negligible above 1 GV. The upper limit of residual contamination in the helium

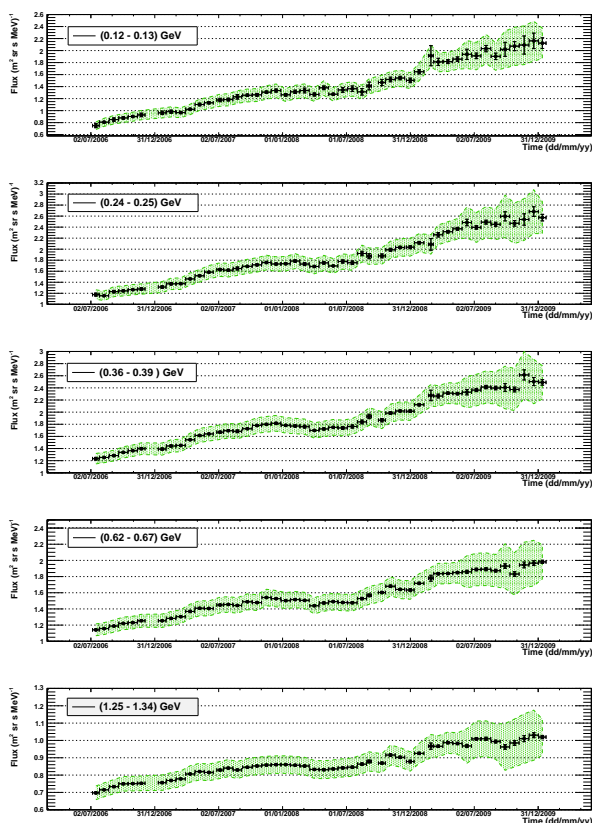


Figure 4: Time dependence of the hydrogen flux as measured by PAMELA in different energy ranges (increasing energy from top to bottom panel).

flux sample was found to be lower than 1% [9]. Finally, a further correction was included in order to account for spectra attenuation due to particles interacting with the satellite and the instrument itself. This effect was slightly energy dependent and amounted, according to simulation, to 5 – 6% for hydrogen and to slightly more than 10% for helium.

PAMELA hydrogen and preliminary helium spectra are reported in Fig. 2, in terms of yearly averages, from 2006 to 2009. The observed increase in particle intensity is clearly visible in both CR species. Thanks to the high collected statistics, the hydrogen particle intensity has been measured for each Carrington rotation¹, going from Carrington rotation number 2045 to number 2092. The data collected between July 2006 and December 2009 are shown in Fig. 3 for several time periods. The error bars and the shadowed regions represent, respectively, the statistical error and the systematic uncertainty. In order to correct for systematic time-dependent variations of the Carrington fluxes, these were normalized at high-energy (30 – 50 GeV) to the proton flux measured with the more stringent tracking conditions of Adriani et al. [1] and averaged over the period July 2006 - March 2008. The assumption behind this correction implies that PAMELA results are not sensitive to solar modulation induced flux variations smaller than about 5%.

For each rigidity bin it has been possible to follow the time evolution of the hydrogen spectrum, as shown in Fig. 4. The increase of the particle absolute intensity with time is compatible with the decreasing solar activity during the solar minimum 2006-2009. In references [10, 11],

PAMELA proton data have been compared with spectra computed using a model based on the numerical solution of the Parker transport equation, including all the major modulation mechanisms (convection, gradient and curvature drifts, diffusion and adiabatic energy changes). This study has led to an improved comprehension of the rigidity dependence of the diffusion coefficient and to a better understanding of the relative contribution of the mentioned modulation mechanisms during the observed solar minimum.

5 Conclusions

The PAMELA experiment orbital and instrumental characteristics and its long time exposure are allowing to measure the hydrogen and helium fluxes with high precision and, thanks to the high statistics collected, to monitor their evolution in time. The absolute low energy proton spectra were found to increase significantly by becoming progressively softer from 2006 to 2009 as solar activity decreases to a very low level. The helium data analysis procedure and preliminary data are also presented. Moreover, additional information on the solar modulation effect can be gathered by using the PAMELA electron and positron data [12, 13] and the data collected from 2009, whose analysis is now ongoing.

References

- [1] O. Adriani, et al., *Science* 332 (2011) 69- doi:10.1126/science.1199172
- [2] O. Adriani, et al., *Astrophys. J.* 765 (2013) 91 doi:10.1088/0004-637X/765/2/91
- [3] M. S. Potgieter, *Living Rev. Solar Phys.* 10, 3 (2013) doi:10.12942/lrsp-2013-3
- [4] R. D. Strauss, et al., *Advances in Space Research* 49 (2) (2012) 392 doi:10.1016/j.asr.2011.10.006
- [5] R. A. Mewaldt, et al., *Astrophys. J.* 723 L1 (2010) doi:10.1088/2041-8205/723/1/L1
- [6] D. G. Cerdano, et al., *Nucl.Phys.B* 854, 3 (2012) 738-779 doi:10.1016/j.nuclphysb.2011.09.020
- [7] P. Picozza, et al., *Astroparticle Physics* 27 (2007) 296-315 doi:10.1016/j.astropartphys.2006.12.002
- [8] G. D'Agostini, *NIM A*362 (1995), 487-498
- [9] N. Nikonov, Ph.D. thesis (2011), University of Rome Tor Vergata, Italy, <http://pamela.roma2.infn.it>
- [10] M. S. Potgieter, et al., *Solar Physics* (2013), in press
- [11] E.E. Vos, et al., ICRC Proceedings, this conference
- [12] R. Munini, et al., ICRC Proceedings, this conference
- [13] E.E. Vos, et al., ICRC Proceedings, this conference

1. Mean synodic rotational period of the Sun surface, corresponding to about 27.28 days